Inherent Self-Interference Cancellation for In-Band Full-Duplex Single-Antenna Systems

Seiran Khaledian *Student Member, IEEE,* Farhad Farzami, *Student Member, IEEE,* Besma Smida, *Senior Member, IEEE,* and Danilo Erricolo, *Fellow, IEEE*

***Abstract*—We propose a new analog self-interference cancellation (SIC) technique for in-band full-duplex transmission (IBFD) in single-antenna systems. We use an RF circulator to separate transmitted (Tx) and received (Rx) signals. Instead of estimating the self-interference (SI) signals and subtracting them from the Rx signals, we use the *inherent* secondary SI signals at the circulator, reflected by the antenna, to cancel the primary SI signals leaked from the Tx port to the Rx port. We modified the frequency response of the secondary SI signals using a reconfigurable impedance mismatched terminal (IMT) circuit, which consists of two varactor diodes at the antenna port. We can also adjust the frequency band and bandwidth by controlling the varactor diodes bias voltages. The IMT adjustability makes it robust to antenna input impedance variations and fabrication errors. We analyze and fabricate a prototype of the proposed technique at 2.45 GHz. We achieved more than 40 dB cancellation over 65 MHz of bandwidth. Our technique is independent of the RF circulator and antenna type and it can be applied to any frequency band. It is also very relevant to small mobile devices because it provides a simple, low-power and low-cost adjustable analog SIC technique.**

***Index Terms*—Analog cancellation, in-band full-duplex, linearity, passive cancellation, reconfigurable mismatched terminal, RF circulator, self-interference cancellation, single-antenna system and varactor diode.**

I. Introduction

In in-band full-duplex (IBFD) communication systems, nodes are able to transmit and receive simultaneously in the same frequency band. IBFD communications have the potential of doubling the spectrum efficiency of communication systems as well as eliminating hidden terminals and the need of duplex filters, improving fairness and network latency [**?**], [**?**], [**?**], [**?**], [**?**], [**?**]. However, IBFD systems suffer from strong self-interference (SI) signals that are imposed on the received (Rx) signals by the transmitted (Tx) signals. Thus, the major challenge that IBFD systems must confront is reducing SI signals. The amount of self-interference cancellation (SIC) value for an efficient IBFD system depends on the Tx signal power and the noise floor at the receiver. The SI signal level should be reduced to the same level as the receiver noise floor [**?**], [**?**]. The main obstacle to cancel out SI signals lies in the fact that they are random and often unpredictable. As the Tx signals go through the digital to analog converter, the up-convert mixer and power amplifier, there are harmonics, linear and nonlinear distortions, extra noise and frequency selective delays that are added to the Tx signals, making them totally different from the original Tx signals at the base-band.

Up to date, many works have proposed different SIC techniques. Recently, the feasibility of a practical IBFD system has been proved [**?**], [**?**], [**?**]. The SIC can be accomplished in three ways: passive cancellation, digital cancellation and analog (RF) cancellation. Passive cancellation uses electromagnetic isolation between Tx and Rx antennas. This method includes physical separation of antennas, directional isolation of antennas, absorptive shielding, polarization diversity, using band-gap structures, inductive loops, wave traps and slots on the ground plane [**?**], [**?**], [**?**]. In digital cancellation, the base-band Tx signals are subtracted from the Rx signals all in digital domain [**?**], [**?**]. Digital cancellation must be applied along with analog cancellation to achieve an efficient SIC. In the analog SIC, sample Tx signals with all transmitter impairments are tapped and manipulated through an estimator circuit to create a replica of the SI signals. This modified Tx sample is called cancellation signals and added to the Rx signals to cancel out SI signals [**?**].

Most of the previous techniques use multiple antennas (at least one Rx and one Tx antenna) [**?**], [**?**], [**?**], [**?**], [**?**], [**?**], [**?**], [**?**], [**?**], [**?**], [**?**]. Using separate antennas significantly increases the SIC level, but it has two main drawbacks: First, using multiple antennas prevents from dense integration of IBFD systems due to the required physical distance of the antennas [**?**]. In other words, it does not satisfy the desired form-factor of most of today's wireless communication systems, see Table 2 of [**?**]. Second, multiple antennas configurations can be used in spatial duplexing system design rather than solving the duplexing problem in frequency or time domain as in IBFD systems [**?**], [**?**], [**?**]. This warrants the study of single antenna IBFD systems.

Fewer works have studied single-antenna IBFD systems compared to multiple antennas configurations. To the best of our knowledge, the first single-antenna IBFD configuration was introduced in [**?**]. It used two lumped-element circulators and two 3 dB quadrature hybrids to reduce SI signals. This configuration achieved up to 40 dB of isolation between Tx and Rx channels over a 25 MHz bandwidth in the 900 MHz frequency band. Unfortunately, it is costly because it needs two RF circulators and the lumped-element microwave components are hard to implement at higher frequencies, due to low quality factor of inductors and capacitors. Recently, the authors of [**?**], [**?**], [**?**] used a complex feed forward network including multiple delay lines, tunable attenuator along with adaptive

This work was partially funded by the US National Science Foundation CAREER award 1620902.

S. Khaledian, F. Farzami, B. Smida and D. Erricolo are with Department of Electrical and Computer Engineering, University of Illinois at Chicago, Chicago, IL, USA. Authors e-mails are : seiran.kh@gmail.com, farzami.farhad@gmail.com, smida@uic.edu and derric1@uic.edu.

TABLE I.
COMPARISON AMONG DIFFERENT SELF-INTERFERENCE CANCELLATION TECHNIQUES AND THIS WORK [†].

Ref	Short description	Complexity / Form-factor	Power consumption	Signal loss	SIC(dB) / f (GHz) / FBW(%)
[?] [?] [?] [?] [?]	Tx power splits up between the antenna and an impedance balance network. Hybrid transformer is used to subtracts the voltage across these impedances.	Average / Large	Low	High	45 / 2.4 / 0.84 50 / 1.95 / - 62 / 1.9 / 1 50 / 2.45 / 0.24 50 / 2.45 / 0.2
[?]	Orthogonal linear polarizations for Tx and Rx + a reconfigurable reflective termination on the auxiliary port that reflects the coupled signal to cancel SI at Rx port.	Average / Large	Average	Average	50 / 4.6 / 6.5
[?]	A feed network of two lumped-element circulators and two 3 dB quadrature hybrids are designed to cancel out the leakage of Tx at the Rx path.	High / Average	Zero	Average	40 / 0.9 / 2.8
[?] [?] [?]	Amplitudes and phases of the sampled Tx signals are modified to create the cancellation signals, which are added to the Rx path to cancel the SI signals.	High / Large	High	Average	60 / 2.4 / 3.3 60 / 2.4 / 0.83 58 / 5.8 / -
[?]	An impedance tuning circuit placed at the coupling port of a directional coupler, is used to generate the reflected signal to cancel out Tx leakage signal.	Average / Large	Low	High	65 / 0.915 / 11
[†]	Using the inherent secondary SI signal at the circulator, to cancel the primary SI signal by means of IMT circuit.	Low / Small	Low	Low	40 / 2.45 / 2.7

algorithm, which is not practical for small cellular devices. An electrical balance duplexer has been used to achieve high SIC in single-antenna IBFD systems in [?], [?], [?], [?], [?]. The main drawback of this technique is the large Tx insertion loss (half of the Tx power is lost). In [?] a simultaneous transmit and receive antenna with two arm pairs (one pair as Tx and one pair as Rx antennas) in one platform has been proposed. A 39.5 dB isolation between Rx and Tx channels has been achieved by using two 3 dB 180° hybrids. However, the achieved isolation only applies to the proposed four-arms antenna and cannot be used for a generic IBFD system. A dual-polarized antenna has been used in [?], [?] and up to 60 dB and 47 dB isolation between Tx and Rx ports have been achieved, respectively. Exploiting orthogonal polarizations is one of the diversity schemes used to increase the capacity in multiple-input and multiple-output (MIMO) systems [?].

The novelty of this article is that we use the circulator *inherent* secondary SI signals reflected by the antenna, to cancel the primary SI signals leaked from the Tx port to the Rx port. This is in contrast to the feed-forward technique which has been widely used in previous studies. We modified the frequency response of the secondary SI signal using an adjustable impedance mismatched terminal (IMT) circuit at the antenna port. Accordingly, our contributions are the following: 1) We introduced a novel and efficient analog SIC technique that uses the RF circulator inherent SI signals and the RF circulator rotation property. This decreases the complexity, cost and power consumption of the SIC circuit by eliminating many RF components (sampler, combiner, attenuator and phase shifter). 2) We proposed a reconfigurable IMT circuit by exploiting two varactor diodes. This increases the system robustness to the antenna input impedance variations, component frequency response deviations and fabrication errors. 3) We fabricated a prototype of single-antenna IBFD system at 2.45 GHz and achieved 40 dB SIC over a 65 MHz bandwidth. Table I summarizes the comparisons between this work and some other state-of-the-art.

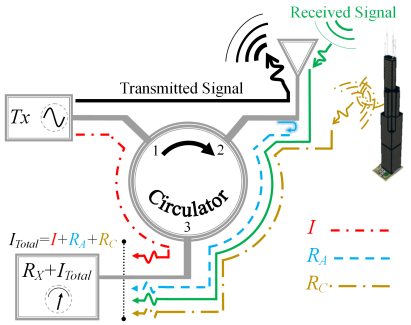

Fig. 1. Single-antenna IBFD communication signal diagram.

The paper is organized as it follows: In Section II, we describe the principle of operation of the proposed inherent SIC technique. In Section III, we present how to build a robust reconfigurable IMT circuit. The simulation and measurement results of a prototype inherent SIC circuit at 2.45 GHz are presented and discussed in Section IV. The system limitation are discussed in this section. Section V concludes the paper.

II. PRINCIPLE OF OPERATION

A. SI Signals in a Single-Antenna IBFD Communication

Fig. 1 shows the signal diagram of a single-antenna IBFD wireless communication system. A single antenna is used for transmitting and receiving. The Tx and Rx channels are separated through an RF circulator. Port 1 of the circulator is connected to the Tx channel and port 3 is connected to the Rx channel. Practically, RF circulators do not provide perfect isolation among their ports, thus some Tx signals leak to the Rx channel, causing the primary inherent SI signals, illustrated by I in Fig. 1. The secondary inherent SI signals are shown by R_A and come from the Tx signals reflected at the antenna due to the inherent impedance mismatch, added to

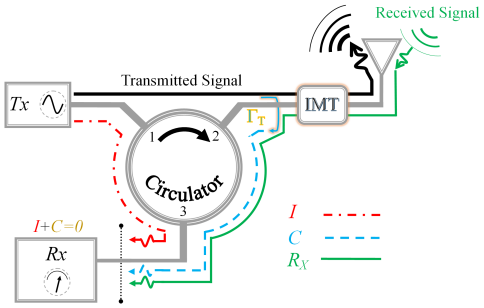

Fig. 2. Single-antenna IBFD system integrated with the IMT circuit.

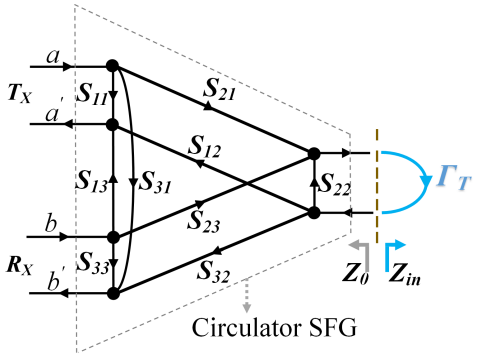

Fig. 3. Signal-flow graph for the signals in Fig. 2.

the receiver through the circulator rotation property. Another SI signal shown by R_C in Fig. 1 is due to environmental scattering.

These interference signals have different amplitudes and phases, depending on the circuit frequency response and the environment parameters. However, I and R_A usually have the highest power because they do not experience path-loss. As shown in Fig. 1, the desired received signal Rx is combined with major SI signals I, R_A and R_C at the receiver. Due to the free space path loss, Rx is significantly weaker than *SI* signals level, which makes it impossible to be extracted at the receiver. Thus, the interference signals must be effectively suppressed at the receiver.

B. Common Analog SI Cancellation Technique

In analog cancellation, we attempt to suppress the SI signals I and R_A. R_C is usually canceled with digital cancellation using pilot sequences and tones [**?**]. The common analog cancellation technique is to tap the Tx signals, modify their amplitude and phase responses, and then add them to the Rx channel. The modified Tx sample is called cancellation signal (C). The cancellation signals have the same amplitude and 180° phase shift compared to the SI signals. In other words, the cancellation signals cancel out SI signals R_A and I to have $Rx + I + R_A + C = Rx$ at the receiver. In the literature, different algorithms and techniques to implement this concept have been proposed and different values of achieved analog SIC have been reported [**?**], [**?**], [**?**].

C. The Proposed Analog SIC Technique

The new analog SIC technique is the following: we use the SI signals R_A as the cancellation signals. This is different from sampling from the Tx channel as in case of previous works. In other words, we take advantage of the reflected Tx signals at the antenna interface. However, the amplitude and phase of R_A must be modified to cancel out I at the receiver. To do so, we add a reconfigurable IMT circuit at the antenna interface to manipulate the amplitude and phase of R_A. Fig. 2 shows the new analog cancellation technique integrated in a single-antenna IBFD system. Here, the amplitude and phase of the cancellation signals are modified through the reflection coefficient Γ_T seen by the IMT circuit. Thus, the IMT circuit is an impedance mismatched circuit, designed to provide the desired Γ_T.

The cancellation signals are then added to the Rx channel using rotation property of the RF circulator. As a result, the cancellation signals are tapped and added to the signals at the receiver without using feed forward architecture. It should be noticed, the proposed technique is not dependent on the RF circulator isolation level. The lower isolation needs more reflection and the higher isolation needs less reflection. However, the RF circulators isolation normally are small enough to maintain the reflection portion negligible. Before investigating the possible configurations of IMT circuit, we need to determine the amplitude and phase of Γ_T to provide the proper cancellation signal.

D. Γ_T derivation

The reflection coefficient Γ_T is derived using the signal-flow graph (SFG) of Fig. 2, illustrated in Fig. 3. The circulator SFG is obtained considering the reflection coefficient, insertion loss, and isolation at each port. S_{11}, S_{22} and S_{33} are the return loss of port 1, 2 and 3 of the circulator, respectively. S_{21}, S_{32} and S_{13} are the insertion loss from port 1 to 2, port 2 to 3 and port 3 to 1, respectively. S_{12}, S_{31} and S_{23} are isolation between port 1 and 3, port 1 and 2 and port 2 and 3, respectively. Z_{in} is the input impedance seen by the IMT circuit interface. a and a' represent the incident and reflected Tx signals while b and b' are the incident and reflected Rx signals respectively. The value of b'/a defines the amount of signal a (Tx) leaking to the Rx port due to circulator leakage and Γ_T. The derivation of b'/a is carried out using Mason's rule [**?**] as follows:

$$\frac{b'}{a} = \frac{S_{31}(1 - \Gamma_T S_{22}) + S_{21}\Gamma_T S_{32}}{1 - \Gamma_T S_{22}}. \tag{1}$$

Now the required Γ_T can be determined by setting (1) equal to zero, resulting in

$$\Gamma_T = \frac{S_{31}}{S_{31}S_{22} - S_{21}S_{32}}. \tag{2}$$

From the definition of the reflection coefficient, we have

$$Z_{in} = \frac{Z_0 + \Gamma_T Z_0}{1 - \Gamma_T}, \tag{3}$$

where Z_0 is the input impedance (characteristic impedance) of the circulator seen at the port 2. The IMT circuit is an impedance matching circuit which transfers the antenna input impedance to Z_{in}. Since $|\Gamma_T| << 1$, transmission and reception losses are negligible.

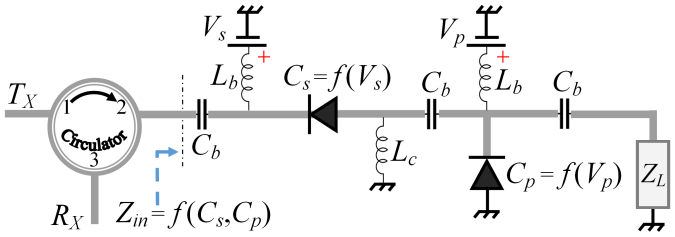

Fig. 4. Schematic of a reconfigurable IMT circuit with parallel and series varactor diodes. Z_L is the antenna input impedance.

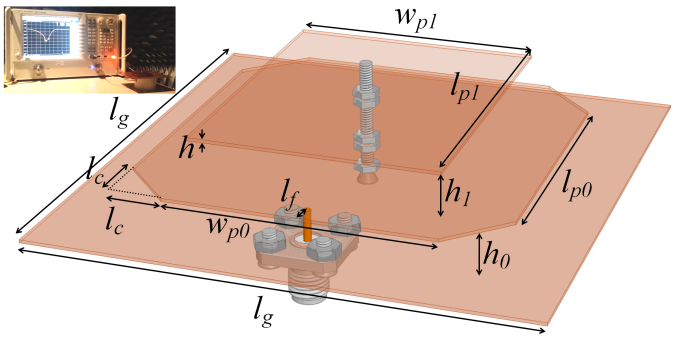

Fig. 5. Air filled stacked patch antenna layout. All dimensions are in mm: $l_g = 120$, $W_{p0} = 44$, $l_{p0} = 43.5$, $W_{p1} = 40.5$, $l_{p1} = 49$, $h_0 = 4.5$, $h_1 = 6.5$, $h_p = 0.5$, $l_c = 5$ and $l_f = 4.5$.

III. Reconfigurable IMT Circuit

This section studies the IMT configuration that delivers the desired Z_{in}. The value of Z_{in} is determined using (2) and (3). However, when it comes to the antenna, the following challenges appear: a) different antennas show different values of input impedance; b) even for a specific antenna, its input impedance varies within its frequency bandwidth of operation; and, c) the input impedance may slightly change due to the fabrication errors or mounting location.

Thus, an adjustable IMT design is needed to compensate for the antenna input impedance variation and also the fabrication errors and other RF components frequency response deviations. We propose a simple impedance mismatched circuit with two degrees of freedom as: a) a variable series capacitance and, b) a variable shunt capacitance. A mismatched circuit with these two degrees of freedom can match the antenna input impedance and tune potential circuit component frequency response deviations to the desired Z_{in}.

Fig. 4 shows the schematic of the proposed IMT circuit with one series and one parallel varactor diodes. In this figure, Z_L represents the antenna input impedance and C_p and C_s are the parallel and series variable capacitance realized by varactor diodes. The varactor diode capacitance is a function of its dc bias voltage, $C_s = f(V_s)$ and $C_p = f(V_p)$. Furthermore, the input impedance of the IMT circuit is a function of C_s and C_p. Thus, we can tune Z_{in} via V_s and V_p. The inductor L_c is connected to the ground to close the dc current path of the series varactor. We used this technique to build a single-antenna IBFD system at 2.45 GHz, described in the next section.

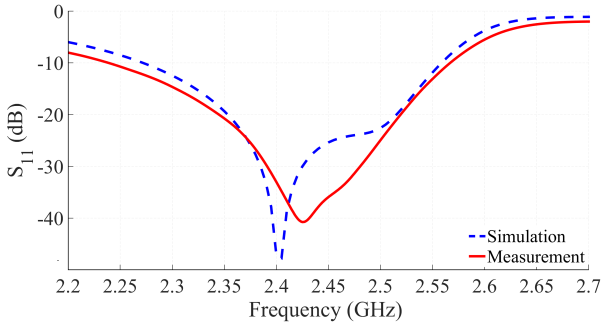

Fig. 6. Simulated and measured S_{11} of the antenna shown in Fig. 5.

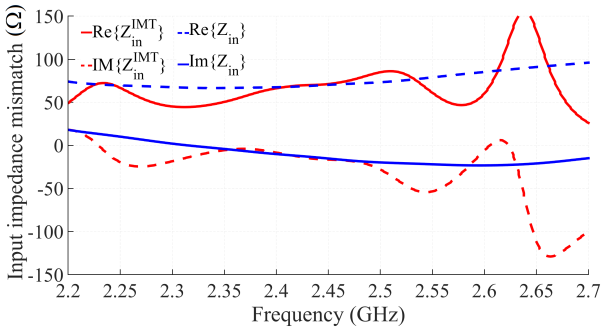

Fig. 7. Real and imaginary parts of Z_{in} corresponding to the circulator CR5853, and Z_{in}^{IMT} of Fig. 8 for $V_p = 3$ V and $V_s = 2.4$ V.

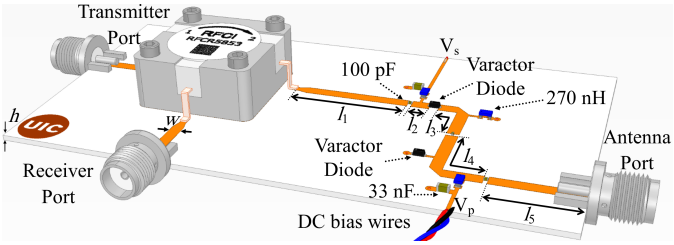

Fig. 8. IMT layout connected to the circulator at 2.45 GHz. The parameter values in mm are: $l_1 = 19$, $l_2 = 3$, $l_3 = 9.5$, $l_4 = 15$, $l_5 = 12.5$ and $W = 1.8$.

IV. Single-Antenna IBFD Prototype at 2.45 GHz

A. Components

This prototype system consists of 3 parts: the antenna, the IMT circuit and the circulator. Each part is analyzed separately.

1) The antenna: We used an air filled stacked patch antenna since it shows a good matching bandwidth and it is easy to fabricate. This type of antenna is also a successful model in the Wi-Fi transmitter market. Fig. 5 shows the layout of the designed antenna at 2.45 GHz. The simulation results from HFSS and S_{11} measurements of the antenna are shown in Fig. 6.

2) The circulator: We used a circulator with part number CR5853 from RFCI. This circulator shows 15.5 dB isolation among its port at 2.45 GHz. The measured circulator S-parameters are substituted in (2) and (3) to derive Z_{in}, which is shown in Fig. 7.

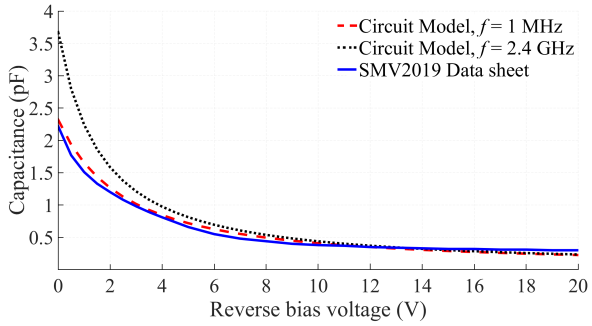

Fig. 9. SMV 2019 varactor diode capacitance values vs. dc bias voltage.

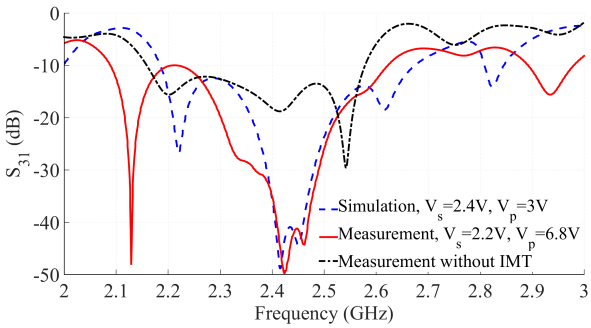

Fig. 10. Wideband analog SIC simulation and measurement performance. The 40 dB cancellation bandwidth is 60 MHz. The Tx-Rx channel isolation is around 15.5 dB without using IMT circuit.

3) The Reconfigurable IMT *Circuit:* The layout of the IMT circuit that operates at 2.45 GHz is shown in Fig. 8 and it follows the considerations explained in Section III.

The series and parallel variable capacitance is implemented using varactor diodes, which should be chosen to have small insertion loss and proper capacitance range. We used varactor diode SMV 2019 from Skyworks Inc. Its *C-V* curve, which shows a slightly dispersive frequency response, is shown in Fig. 9. The circuit model provided by Skyworks is used for the circuit simulation with Advanced Design Systems (ADS) from Keysight.

The substrate is R04003C from Rogers with $\epsilon_r = 3.55$ and $h = 0.8128$ mm (32 mil). The dc bias capacitors are from Murata and the inductors are from Coilcraft. The IMT circuit simply includes microstrip transmission lines with two varactor diodes in series and parallel configuration. The dc bias lines feed the varactor diodes and have been separated from the RF signals by proper RF chokes. The meander line keeps the circuit low profile. To improve the simulation accuracy, the electromagnetic co-simulator of ADS was used. The circuit is designed by setting the dc bias voltages of the varactor diodes in the middle of their capacitance range for tuning purposes after fabrication. The simulated input impedance of the designed IMT circuit is shown in Fig. 7. The real and imaginary parts of the IMT circuit impedance are matched for the required Z_{in} at 2.45 GHz.

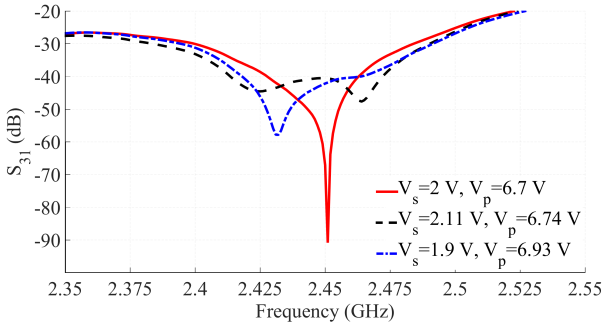

Fig. 11. Different measurement results of achieved SIC, corresponding to different sets of varactor diodes dc bias voltages.

B. Simulation and Measurement Results

We evaluate the final performance of the single-antenna IBFD system by measuring the achieved SI cancellation. Thus the amount of Tx signal leaked to the receiver (S_{31}) is measured using an Agilent N5222A PNA Vector Network Analyzer. However, since the input impedance of IMT circuit is a function of the varactor diodes dc bias voltages, the proposed SIC technique provides various *SIC* levels for different sets of V_p and V_s. Based on the application, we can set the dc biases to have a high amount of SI cancellation and/or a wideband spectrum SIC. We also can adjust the operating frequency using V_p and V_s. For example, for $V_p = 6.8$ V and $V_s = 2.2$ V, a 40 dB analog SI cancellation over 60 MHz of frequency bandwidth has been achieved, as shown in Fig. 10. As discussed earlier, the input impedance of the antenna connected to the IMT circuit (Z_{in}^{IMT}) should match Z_{in} over the desired frequency bandwidth. As shown in Fig. 7, Z_{in}^{IMT} follows Z_{in} at 2.45 GHz over the 60 MHz frequency bandwidth where SI cancellation occurs.

The SIC performance is also measured for other dc voltage bias sets. Fig. 11 shows the achieved cancellation for three extra dc bias voltages. A 65 MHz frequency bandwidth with 40 dB SIC is achieved using $V_s = 2.1$ V and $V_p = 6.8$ V. We shifted the operation frequency from 2.45 GHz to 2.43 GHz using $V_s = 1.9$ V and $V_p = 7$ V. The measured results of Fig. 11 shows that the final performance of the single antenna IBFD system, can be controlled with V_p and V_s. The measured insertion loss is 0.75 dB, which is negligible compared to other analog cancellation techniques used in previous works, and applies to both the Tx to antenna path and the antenna to Rx path. The maximum dc power consumption of each varactor diode, considering the maximum reverse current of 20 nA, is around 0.15 mW. It is noteworthy that the amount of SIC achieved using this technique is sufficient to make sure that the Rx channel is not saturated by the Tx signal. This technique should be combined with a digital cancellation stage to form a practical IBFD system.

C. Dynamic Algorithm for SIC in a Practical Scenario

We provide a practical algorithm for a real time communication scenario since monitoring the *SI* signal level is essential for the performance of a full-duplex system. The SI

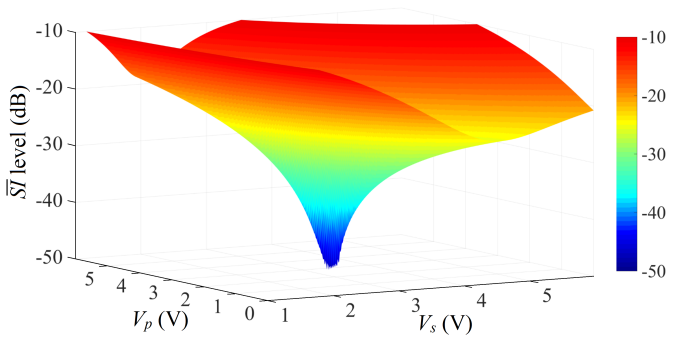

Fig. 12. $\overline{SI}$ level in $f \in (2.41, 2.47)$ GHz based on variable voltages $1\text{ V} < V_s < 6\text{ V}$ and $0\text{ V} < V_p < 6\text{ V}$.

signals can be monitored by sending pilot signals and detecting them at the Rx port. In addition, the *SI* signals level can be minimized by changing the varactor diodes bias voltages and, in particular, we apply the *direct pattern search* [**?**] to optimize them. Note that with inherent SIC technique, we use the SI signal inside the circulator. The channel propagation variation inside the circulator is very slow (compared to Tx-Rx channel propagation). Hence, the tuning of the varactor diode bias voltage should be done occasionally and may stay optimal over many transmitted packets. As an example, we consider the 60 MHz bandwidth from 2.41 GHz to 2.47 GHz. Within this bandwidth, the goal of the algorithm is to minimize the average *SI* ($\overline{SI}$) level, which is shown in Fig. 12.

The algorithm steps are as follows:

i) Set $V_s = V_1$ V, $V_p = V_2$ V and the $\overline{SI}$ level goal.

ii) Send pilot signals and measure $\overline{SI}$ level at the four points $(V_s = V_1 \pm \delta, V_p = V_2)$ V and $(V_s = V_1, V_p = V_2 \pm \delta)$ V.

iii) Find the minimum $\overline{SI}$ level among four measurements and update the varactor diodes voltages.

iv) Compare the minimum $\overline{SI}$ level just found with the goal. If the goal is achieved or the number of iterations has exceeded the maximum then terminate the search.

v) Otherwise, if the updated voltages did not change, set $\delta = \delta/2$ or set $\delta = \delta_{\min}$ if $\delta < \delta_{\min}$ otherwise do not change δ and go back to step *ii*.

Assume the goal is to achieve $\overline{SI} \leq -45$ dB in the target frequency band. A graphical representation of the path followed by the algorithm as it searches the optimal values is shown in Fig. 13.

The initial step k_0 starts at $(V_1, V_2) = (1, 1)$ V with $\delta = 1$ V and $\delta_{min} = 0.125$ V, see Fig. 13(a). By applying the algorithm, the minimum average SI level is tracked at each step (red markers in Fig. 13) and the goal is achieved at k_{26}.

D. Linearity, Power Handling and Time Response Limitation

The non-linearity effects of the varactor diode on our proposed system is discussed in this section. In the receiving mode, the Rx power level is lower than the level of the varactor diode's non-linear region. However, the Tx power is large and it may limit the linearity of the system. The third order intermodulation distortion (IMD_3) products ($2f_1 - f_2$ and $2f_2 - f_1$) of two fundamental tones at f_1 and f_2 and its third-order intercept point IP_3 is considered as an RF device linearity figure of

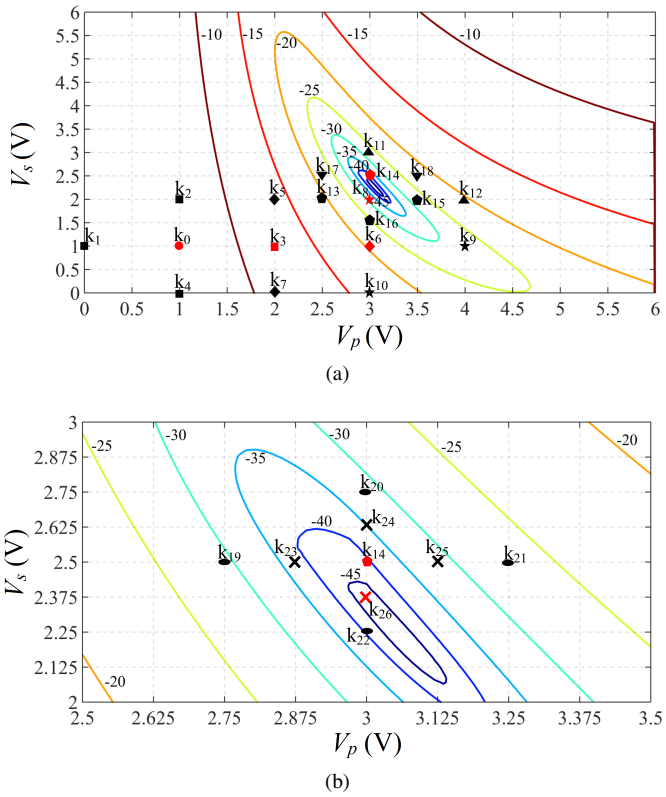

Fig. 13. Example of the direct pattern search algorithm with initial values $V_1 = V_2 = 1$ V, $\delta = 1$ V and $\delta_{min} = 0.125$ V. The contour values are the average *SI* levels. (a) Algorithm steps up to step 14th and (b) a magnified view of the remaing steps until the goal is achieved. Same markers show the same cluster and the red ones show the minimum one.

merit. IP_3 can be read with reference to the input power IIP_3 or to the output power OIP_3, which are almost the same in our case. In particular, $IIP_3(\text{dBm}) = P_{in}(\text{dBm}) - 0.5IMD_3(\text{dBc})$ [**?**].

To evaluate the varactor diode SMV 2019 linearity limitation, we simulated the diode model in ADS. The fundamental tones have 1 MHz offset from the center frequency at 2.45 GHz with 15 dBm input power. The varactor diode bias voltage is 2.5 V which is about the voltage values to achieve the maximum SIC level. The results show $IMD_3 = 47$ dBc and $IIP_3 = 37.5$ dBm.

In order to validate the simulation results, we fabricated an evaluation board to measure the varactor diode IMD_3, see the inset of Fig. 14(a). The input spectrum of the fundamental tones is monitored to see if the measurement set up is clean from harmonics, Fig. 14(a). $IMD_3 = 45.6$ dBc that shows a very good agreement with the simulation results and it is acceptable for wireless communication purposes, see Fig. 14(b). The measurement results for IIP_3 are around 37 dBm. Since the proposed technique is independent of the varactor diode types, other types of varactor diodes with better performance may be used. We also measured the IMD_3 level of the IMT circuit, Fig. 15. The IIP_3 level is almost the same as one varactor diode measurement result.

The maximum absolute power handling capability is around

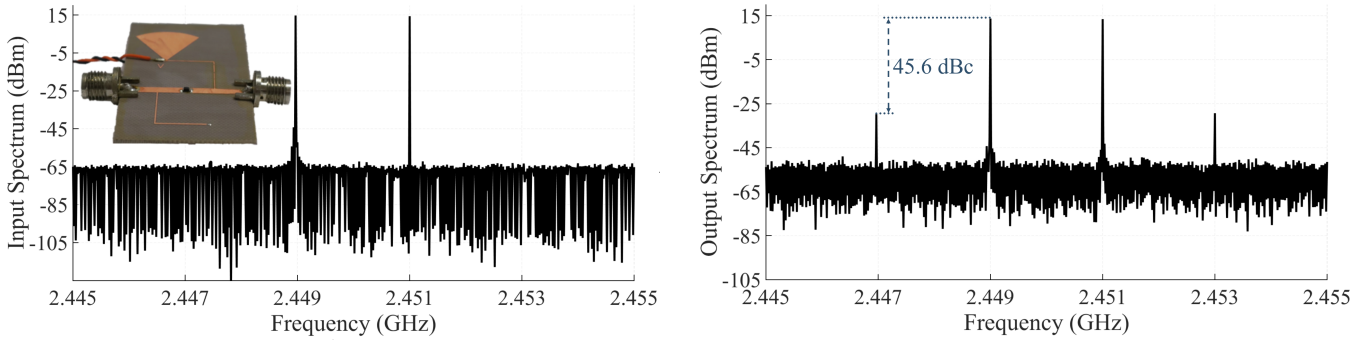

Fig. 14. (a) Evaluation board for IMD_3 measurements and the input fundamental tones and (b) The output spectrum of the varactor diode.

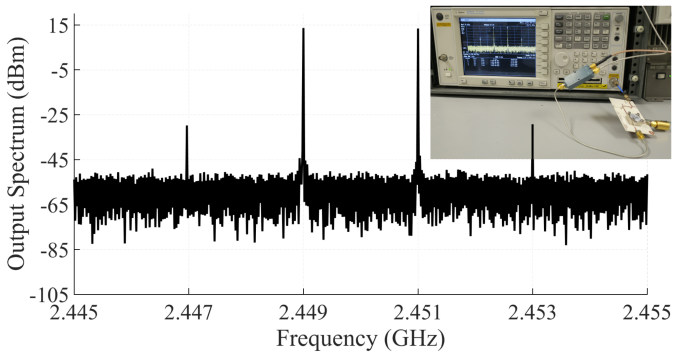

Fig. 15. IMD_3 measurement setup of IMT circuit. The bias voltages are the same as the voltages shown in Fig. 10.

33 dBm for the varactor diode. The measurement are done with 0 dBm input power in the network analyzer. However, the varactor diode capacitance value can be altered by the high input power. The *SI* level at the center frequency of 2.45 GHz vs. the transmitter power measurement shows that the *SI* level is maintained under 40 dB up to around 18 dBm of input power with the initial bias voltages. The voltages may need to be tuned to compensate for this effect for higher input power. It should be noticed that the non-linear products from the high Tx signal power may remain an issue, since they will be above the noise level and should be considered in the digital cancellation stage.

The varactor diode time response is the other limitation factor. The level of *SIC* is a function of the varactor capacitance value. As a result, the diode voltage settling time should be considered. We simulated the unit step response of the diode. The diode voltage variation is less than 1% for $\mathrm{t} > 1.5$ ns. This time delay is very small compared to the data rate for 65 MHz bandwidth. As a result, it does not degrade the communication speed and also it makes the introduced algorithm to run fast.

V. CONCLUSION

We presented a novel analog SI cancellation technique, named inherent SIC. This technique is used in single-antenna IBFD communication systems to cancel out the strong Tx interference imposed on the Rx channel. Contrary to analog cancellation techniques used in other works, here we did not tap from the Tx chain to generate the cancellation signal. We used the secondary inherent SI signal (R_A) to cancel out the primary inherent SI signal (I).

This technique is implemented using an impedance mismatched terminal (IMT) between antenna and circulator. By using the inherent signal rotation path property of the circulator, we eliminate the RF combiner, RF attenuator and RF phase shifter, thus reducing complexity and cost. Inherent SIC circuit is simple with low profile configuration and significantly low power consumption (up to 0.2 mW).

Our design is also robust to antenna input impedance variations and can compensate for fabrication errors and component frequency response deviations by tuning the varactor diodes dc voltage biases. We experimentally showed that our design can show flexible performance depending on the application. As an example, we achieved more than 40 dB of cancellation over 65 MHz of bandwidth. The direct pattern search algorithm is introduced to optimize the SIC level in a practical communication scenario and the varactor diode limitations are discussed to address the practical implementation challenges.

Seiran Khaledian (S'11) received her B.S. degree in electrical engineering from Khaje Nasir University of Technology (KNTU) in 2010 and M.S degree in telecommunication engineering from Tarbiat Modares University in 2013, Tehran, Iran. She is currently a Ph.D. student at the University of Illinois at Chicago (UIC). She is a member of the Networks Information Communications and Engineering Systems Laboratory (NICEST) at the UIC. Her research interests are in realization of 5G wireless communication systems, including full-duplex communication systems, analog self-interference cancellation techniques and reconfigurable antenna and RF/microwave components.

Farhad Farzami (S'10) is a Ph. D. student of Electrical and Computer Engineering at the University of Illinois at Chicago (UIC), Chicago, Illinois, USA. He obtained the B. Sc. from University of Tabriz, Tabriz, Iran in 2009 and M. Sc. from Tarbiat Modares University, Tehran, Iran in 2012.

He joined the Andrew Electromagnetics Lab at UIC in 2014 where he is perusing his Ph. D. His research interests include active and passive front-end microwave circuits and antennas. His research projects include metamaterial based RF circuits for realizing uni-axial propagation media and antenna miniaturization by using ultra-thin magneto-dielectric substrates, backscatter communication for full-duplex and RFID applications, reflection amplifiers, analog self-interference cancellation circuits and reconfigurable antennas for software defined radio applications.

Besma Smida ((S'98–M'06–SM'10) is an Associate Professor of Electrical and Computer Engineering at University of Illinois at Chicago. After completing her appointment as a Postdoc and later a Lecturer at Harvard University, she became an Assistant Professor of Electrical and Computer Engineering at Purdue University Calumet. Additionally, she was a Research Engineer in the Technology Evolution and Standards group of Microcell, Inc. (now Rogers Wireless), Montreal, Canada. Dr. Smida took part in wireless normalization committees (3GPP, T1P1). She obtained the Ph. D. and M. Sc. from the University of Quebec (INRS), Montreal, Canada. Her research focuses on wireless communication theory. She received the Academic Gold Medal of the Governor General of Canada in 2007 and the NSF CAREER award in 2015.

Danilo Erricolo (S'97-M'99-SM'03-F'16) received the Laurea degree of Doctor (summa cum laude) in electronics engineering from the Politecnico di Milano, Milan, Italy, in 1993 and the Ph.D. degree in electrical engineering and computer science from the University of Illinois at Chicago (UIC), Chicago, Illinois, USA, in 1998. He is a Professor in the Department of Electrical and Computer Engineering, UIC, the Director of the Andrew Electromagnetics Laboratory, an adjunct Professor of Bioengineering and in 2017 he was nominated a University of Illinois Scholar. During summer 2009, he was an Air Force Faculty Fellow at the Air Force Research Laboratory, Wright-Patterson Air Force Base, Dayton, Ohio, USA. He has authored or coauthored more than 260 publications in refereed journals and international conferences. He has served as Associate Editor of the IEEE Antennas and Wireless Propagation Letters (2002-2014), the IEEE Transactions on Antennas and Propagation (2013–2016) and Radio Science (2014-2016). In 2006, he was the Guest Editor of the Special Issues on RF Effects on Digital Systems of the Electromagnetics Journal, and in 2012 he was the Lead Guest Editor of the Special Issue on Propagation Models and Inversion Approaches for Subsurface and Through Wall Imaging, of the International Journal of Antennas and Propagation. His research interests are primarily in the areas of electromagnetic propagation and scattering, high-frequency techniques, wireless communications, electromagnetic compatibility, the computation of special functions, and magnetic resonance imaging.

Dr. Erricolo is a Fellow of IEEE, a member of Eta Kappa Nu and was elected a Full Member of the U.S. National Committee (USNC) of the International Union of Radio Science (URSI) Commissions B, C, and E. He served as Chair (2009- 2011), Vice Chair (2006-2008) and Secretary (2004-2005) of the USNC-URSI Commission E on Electromagnetic Environment and Interference. Between 2009 and 2014, he served as Chair of the USNC-URSI Ernest K. Smith Student Paper Competition. He also served as Vice-Chair of the Local Organizing Committee of the XXIX URSI General Assembly, held in Chicago, Illinois, USA in August 2008. He served as Member at Large of USNC-URSI (2012-2017), a committee of the US National Academies. He was the General Chairman of the 2012 IEEE International Symposium on Antennas and Propagation and USNC-URSI National Radio Science Meeting, held in Chicago, Illinois, USA in July 2012. Between 2011 and 2016, was Chair of the Chicago Joint Chapter of the IEEE Antennas and Propagation Society (AP-S) and Microwave Theory and Techniques Society (MTT). He served on the IEEE AP-S Future Symposia Committee and on the IEEE AP-S/USNC-URSI Joint Meetings Committee (2006-2017 as a USNC-URSI representative). He was an Elected Member of the Administrative Committee of the IEEE AP-S (2012-2014) and served as Chair of the Distinguished Lecturer Program of the IEEE AP-S (2015-2016). He has served on more than 40 conference technical program committees, chaired over 60 conference sessions, and organized more than 20 special sessions at international scientific conferences.